TECHNICAL RESEARCH REPORT

A New Class of Six-Bar Mechanisms with Symmetrical Coupler Curves

by W-B. Shieh, L-W. Tsai,
S. Azarm, A.L. Tits

T.R. 96-51

INSTITUTE FOR SYSTEMS RESEARCH

Sponsored by
the National Science Foundation
Engineering Research Center Program,
the University of Maryland,
Harvard University,
and Industry

Proceedings of
The 1996 ASME Design Engineering Technical Conference and
Computers in Engineering Conference
August 18-22, 1996, Irvine, California

96-DETC/DAC-1116

A NEW CLASS OF SIX-BAR MECHANISMS WITH SYMMETRICAL COUPLER CURVES

W.-B. Shieh[1]
Department of Mechanical Engineering
University of Maryland
College Park, Maryland, 20742

L.-W. Tsai[2]
Department of Mechanical Engineering and
Institute for Systems Research
University of Maryland
College Park, Maryland, 20742

S. Azarm[3]
Department of Mechanical Engineering
University of Maryland
College Park, Maryland, 20742

A.L. Tits[4]
Department of Electrical Engineering and
Institute for Systems Research
University of Maryland
College Park, Maryland, 20742

ABSTRACT

A new class of six-bar mechanisms with symmetrical coupler-point curves is presented. This class of mechanisms is made up of a four-bar linkage with an additional dyad to form an embedded regular or skew pantograph. Because the coupler curve generated at an output point is amplified from that of a four-bar, a compact mechanism with a relatively large coupler curve can be obtained. In addition, due to their structure arrangement, the analysis and synthesis of such mechanisms can be easily achieved. It is shown that the admissible range of transmission angle for such mechanisms is smaller than that of a four-bar mechanism. It is also shown that mechanisms with an embedded skew pantograph exhibit better design flexibility than those with an embedded regular pantograph. Finally, an example mechanism from this class is illustrated and compared with a four-bar linkage with the same coupler curve.

NOMENCLATURE

n Amplification factor of a regular or skew pantograph.

α Crank angle measured counter-clockwise from baseline A_0B_0.

ϵ Minimum transmission angle.

μ Transmission angle of a four-bar mechanism.

ν Transmission angle of the embedded regular pantograph.

ν' Transmission angle of the embedded skew pantograph (type A mechanism).

ν'' Transmission angle of the embedded skew pantograph (type B mechanism).

ρ Size factor of a regular or skew pantograph.

ϕ Coupler plate angle ($=\angle ABC$) of a four-bar mechanism.

ϕ' Coupler plate angle ($=\angle ABG$) of a type A mechanism with an embedded skew pantograph.

ψ_1 Skew pantograph angle ($=\angle HFD$), see Fig. 5.

ψ_2 Skew pantograph angle ($= \angle HDF$), see Fig. 5.

1 INTRODUCTION

It is well known that symmetrical coupler curves can be generated by a four-bar linkage with a coupler link AB and a follower B_0B of equal length, $\overline{AB} = \overline{B_0B}$, as shown in Fig. 1. The coupler point generating a symmetrical curve lies on

[1]Graduate Student
[2]Professor
[3]Associate Professor
[4]Professor

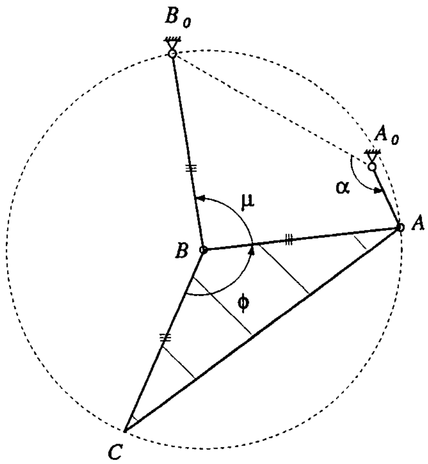

Figure 1. Four-bar linkage with $\overline{AB} = \overline{BC} = \overline{B_0B}$

the circle centered at B and passing through A (Hartenberg and Denavit, 1964). Unlike the four-bar linkage, there are only a few studies on symmetrical coupler curves associated with six-bar linkages. For examples, sufficient conditions for the Watt-I mechanisms with symmetrical coupler curves were investigated by Dijksman (1976; 1980a; 1980b; 1981; 1984). Stephenson-I and -III mechanisms that generated symmetrical coupler curves were reported by Dijksman (1979) and Antuma (1978), respectively. All of the above mechanisms were developed with the use of a four-bar linkage with a symmetrical coupler curve. Among them, most were derived according to Roberts-Chebychev cognate theorem, while others were developed from the Chebychev's dyad or a combination of the two.

Although these six-bar mechanisms all generate symmetrical coupler curves, their characteristics are different from one another. For example, using a four-bar linkage as the source linkage, Hain's six-bar mechanism can trace a symmetrical coupler curve at any point on its translational coupler link (Dijksman, 1976). Note that Hain's six-bar coupler curve is identical to that of the source four-bar. Using the Kempe's over-constrained focal mechanism as the source mechanism, Dijksman's Watt-I mechanism can generate a series of symmetrical curves at various points of its floating link (Dijksman, 1984). A Stephenson-III mechanism derived from the Chebychev's dyad is capable of generating a symmetrical curve whose order is higher than that of a four-bar linkage (Antuma, 1978). Although the abovementioned six-bar linkages are capable of tracing symmetrical coupler curves, none is capable of amplifying the four-bar coupler curve.

In this paper, we present a new class of six-bar linkages made up of a four-bar mechanism with an embedded regular or skew pantograph. This class of six-bar mechanisms are capable of generating amplified symmetrical four-bar coupler curves at their output points. This is particularly useful in applications such as walking machine leg mechanisms for which a compact mechanism with a relatively large output coupler curve is needed (Funabashi et al., 1985, Shieh et al., 1995). Furthermore, unlike the Funabashi's leg design (Funabashi et al., 1985) that uses a general six-bar mechanism, the analysis or synthesis of a six-bar mechanism with an embedded regular or skew pantograph can be easily accomplished in two steps. First, a four-bar linkage is analyzed or synthesized with a desired coupler curve. This is then followed by adding a dyad to form an embedded pantograph. In this way, the analysis or synthesis of the six-bar is essentially simplified to that of a four-bar.

The balance of this paper is organized as follows. In Section 2, the construction of a new class of six-bar linkages with an embedded regular and skew pantograph is described. In Section 3, mechanism characteristics such as the transmission angles and the coupler curves are investigated. In Section 4, an example mechanism is given to demonstrate the capability of such six-bar linkages. In Section 5, we summarize the main results of this study.

2 CONSTRUCTION OF SIX-BAR MECHANISMS WITH SYMMETRICAL COUPLER CURVES

The basic idea for creating a new class of six-bar mechanisms with symmetrical coupler curves is to combine the functions of a four-bar linkage and a pantograph into one. Since there are four links in each of the four-bar mechanism and the pantograph, it is necessary for these two mechanisms to share two common links. By embedding a pantograph in a six-bar linkage, the coupler curve of a four-bar linkage can be amplified at the output point. As it will be described in more details, two different types of six-bar linkages with an embedded regular or skew pantograph are possible. For type A mechanisms, the upper link of the embedded pantograph is a new link passing through B_0 and is parallel to line BC of the four-bar linkage shown in Fig. 1, while the lower link is parallel to the rocker link BB_0. On the other hand, for type B mechanisms, the upper link of the embedded pantograph is the extension of the rocker link, while the lower link is parallel to line BC.

2.1 Construction of Six-Bar Mechanisms with an Embedded Regular Pantograph

In what follows, we first review the function of a regular pantograph. Then, the constructions of types A and B six-bar linkages are described.

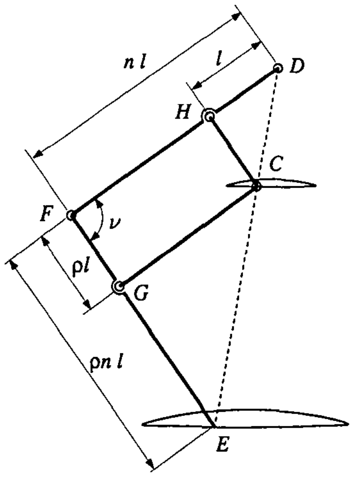

Figure 2. Regular pantograph

2.1.1 Description of a Regular Pantograph. A pantograph is usually used to amplify an input curve at its output point. Referring to the pantograph shown in Fig. 2, points D, C, and E always remain collinear and points H, C, G, and F form a parallelogram. The link lengths of a pantograph are related by two factors n and ρ, where n refers to an amplification factor, while ρ, a size factor, only effects the size of the pantograph.

Provided that point D is fixed and C traces an input curve, point E will trace a similar curve which is amplified by a factor n with respect to the input curve without changing its orientation as shown in Fig. 2. On the other hand, if point C is fixed and point D traces an input curve, point E will trace a similar curve which is amplified by a factor $(n-1)$, and rotated by an angle of π about point C.

2.1.2 Construction of Type A Mechanisms. For type A mechanisms as shown in Figs. 3(a), (b), and (c), the embedded pantograph is B_0HFGEC, and points C and E are the input and output points, respectively. The construction of such mechanisms is carried out through the following steps:

1. Construct a four-bar linkage $A_0 - ABC - B_0$ such that $\overline{AB} = \overline{BC} = \overline{B_0B}$.
2. Starting from point B_0, draw a dashed-line passing through point C.
3. Construct a four-bar parallelogram B_0BGF by adding two binary links B_0F and FG such that $B_0F \| BG$ and $FG \| B_0B$. (The length of B_0F is determined by the amplification factor n.)
4. Locate the intersection point E between the extended lines of B_0C and FG and extend link FG to FE.

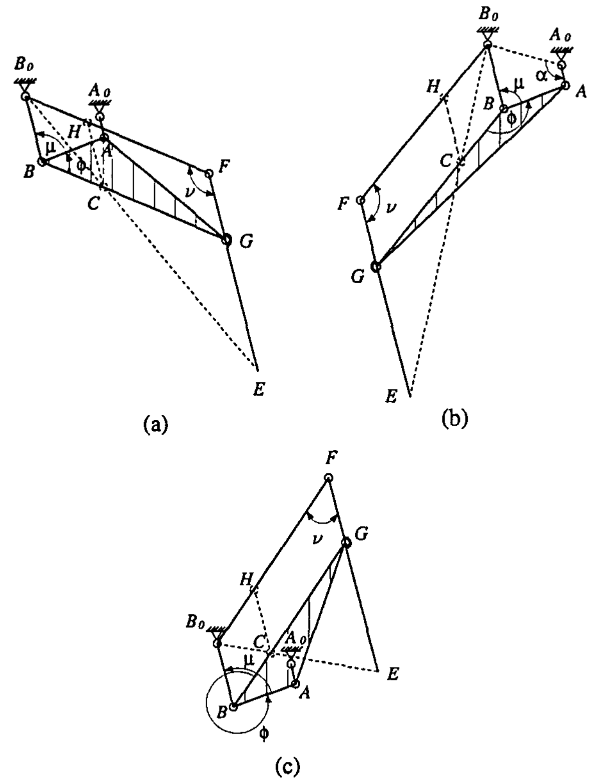

Figure 3. Type A six-bar linkages with an embedded regular pantograph: (a) $0 < \mu + \phi < \pi$;**(b)** $\pi < \mu + \phi < 2\pi$; **(c)** $2\pi < \mu + \phi < 3\pi$.

5. Reshape the coupler plate from ABC to ABG.

For this type of mechanisms, if point B_0 is considered as two concentric binary pivots, then the mechanism becomes a special case of the Stephenson-III mechanism. Referring to the mechanism shown in Fig. 3(b), if link B_0B is replaced by a parallel link of the same length, e.g., link CH, a Stephenson-II mechanism is obtained. If link B_0F of Fig. 3(b), instead of link B_0B, is replaced by a parallel link of the same length, then a Watt-I mechanism is obtained.

For this type of six-bar linkages, the size factor $\rho = 1$ and the link lengths are related by:

$$\overline{B_0F} = \overline{BG} = \overline{FE} = n\,\overline{B_0B} \quad \text{and} \quad \overline{FG} = \overline{B_0B} \tag{1}$$

2.1.3 Construction of Type B Mechanisms. For type B mechanisms as shown in Figs. 4(a), (b), and (c), the embedded regular pantograph is B_0BFGEC and points C and E are the input and output points, respectively. Type B mechanisms are constructed through a similar (as in type A) procedure:

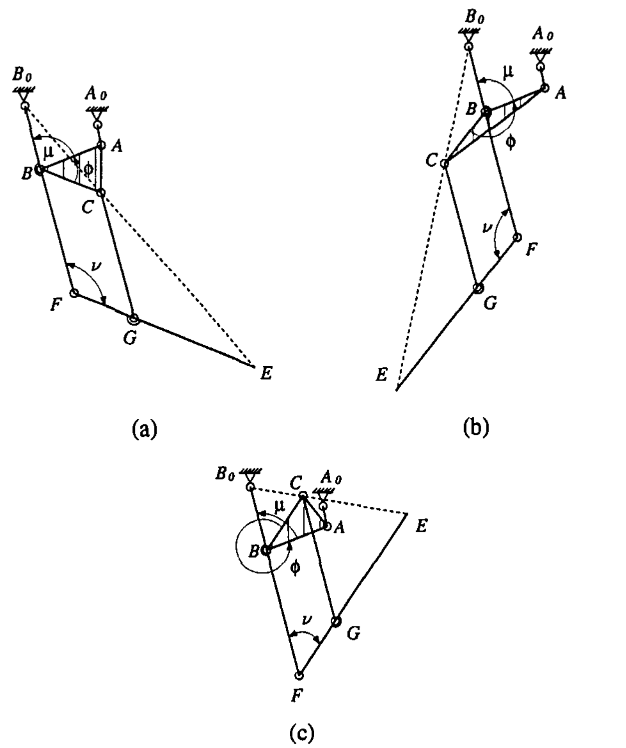

Figure 4. Type B six-bar linkages with an embedded pantograph: (a) $0 < \mu + \phi < \pi$;(b) $\pi < \mu + \phi < 2\pi$; (c) $2\pi < \mu + \phi < 3\pi$.

1. Construct a four-bar linkage $A_0 - ABC - B_0$ such that $\overline{AB} = \overline{BC} = \overline{B_0B}$.
2. Starting from point B_0, draw a dashed-line passing through point C.
3. Extend the rocker link from B_0B to B_0F. (The choice of joint F is determined by the amplification factor n.)
4. Add a binary link FE such that $\overline{FE} \parallel \overline{BC}$. ($E$ is the intersection of $\overrightarrow{B_0C}$ and $\overrightarrow{FE}$.)
5. Create a binary link CG to connect the coupler plate ABC and link FE at points C and G, respectively, such that $\overline{CG} \parallel \overline{BF}$.

For this type of mechanisms, the size factor $\rho = 1$ and the link lengths are related by:

$$\overline{BF} = \overline{CG} = (n-1)\,\overline{B_0B} \quad \text{and} \quad \overline{B_0F} = \overline{FE} = n\,\overline{B_0B} \quad (2)$$

Note that, type B mechanisms are Watt-I mechanisms.

2.2 Six-Bar Mechanisms with an Embedded Skew Pantograph

In this section, we first review the function of a skew pantograph. Then, the constructions of types A and B six-bar mechanisms are described.

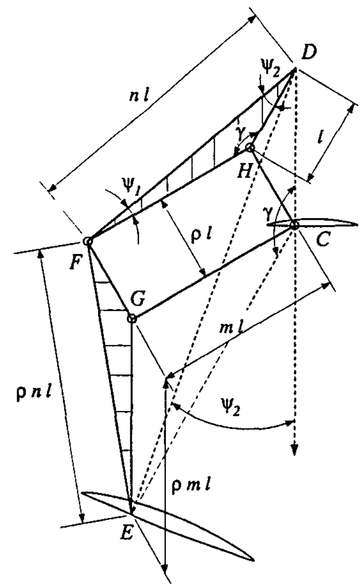

Figure 5. Skew pantograph

2.2.1 Description of a Skew Pantograph.

Referring to the skew pantograph shown in Fig. 5, points H, C, G, and F form a parallelogram and the triangular link DHF is similar to FGE. It is shown (Song et al., 1987) that if point D is fixed and point C traces a given curve, then point E will trace a similar curve which is amplified by a ratio n, and rotated clockwise about the fixed point D through an angle ψ_2 with respect to the given curve as shown in Fig. 5. On the other hand, if point C is fixed and point D traces a given curve, then point E will trace a similar curve which is amplified by a ratio m, and rotated counter-clockwise about the fixed point C through an angle γ, where

$$m = (n^2 - 2n\cos\psi_2 + 1)^{1/2} \quad \text{and} \quad \gamma = \sin^{-1}\left(\tfrac{n\sin\psi_2}{m}\right) \quad (3)$$

Note that, in Fig. 5, ρ effects the size of a skew pantograph.

2.2.2 Construction of Type A Mechanisms.

For type A mechanisms as shown in Figs. 6(a), (b), and (c), the embedded pantograph is B_0HFGEC where point B_0 is a fixed pivot while C and E are the input and output points, respectively. The construction of type A linkages is carried out through the following steps:

1. Construct a four-bar linkage $A_0 - ABC - B_0$ such that $\overline{AB} = \overline{BC} = \overline{B_0B}$.
2. Add a binary link B_0F. (Note that, the length of link B_0F determines the amplification factor while the ori-

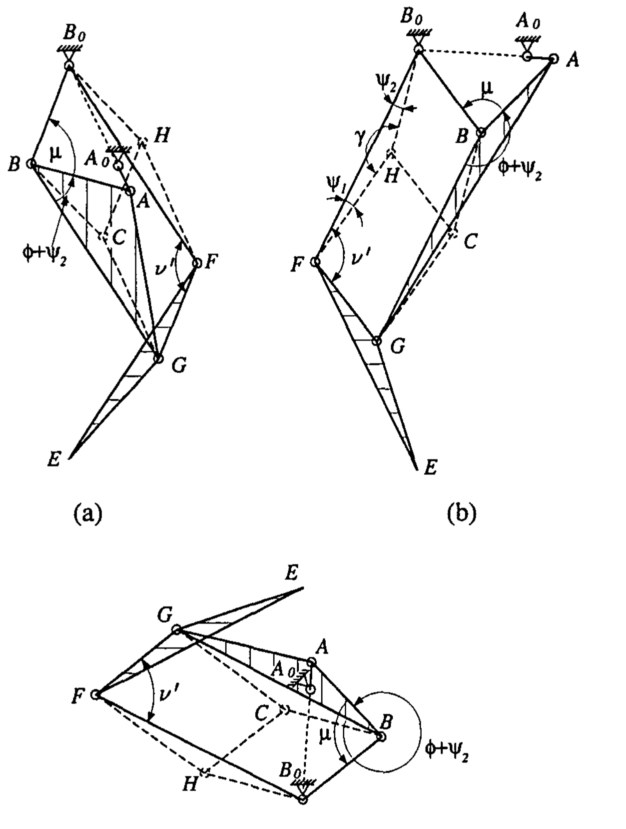

Figure 6. Type A six-bar linkages with an embedded skew pantograph: (with $\phi' = \phi + \psi_2$) (a) $0 < \mu + \phi' < \pi$; (b) $\pi < \mu + \phi' < 2\pi$; and (c) $2\pi < \mu + \phi' < 3\pi$.

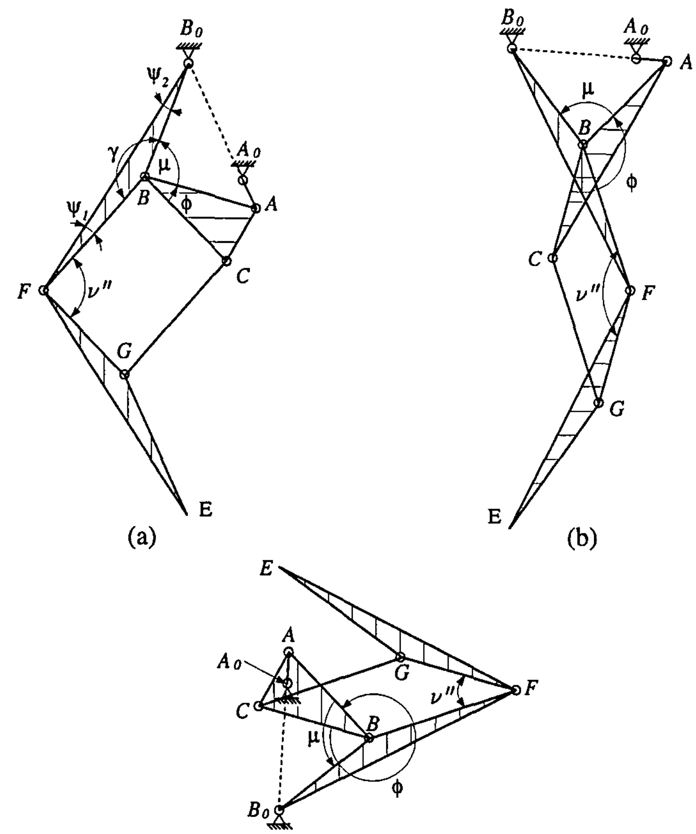

Figure 7. Type B six-bar linkages with an embedded skew pantograph: (with $\phi'' = \phi - \psi_1 - \psi_2$) (a) $0 < \mu + \phi'' < \pi$; (b) $\pi < \mu + \phi'' < 2\pi$; and (c) $2\pi < \mu + \phi'' < 3\pi$.

entation of link B_0F determines the orientation of the output curve.)

3. Form a four-bar parallelogram B_0BGF by reshaping the coupler plate from ABC to ABG and adding a binary link FG.
4. Reshape link FG to a triangular plate FGE such that ΔFGE is identical to ΔBCG.

For this type of mechanisms, if point B_0 is considered as two concentric binary pivots, then such a mechanism becomes a special case of Stephenson-III mechanism. If link B_0B is replaced by a parallel link of the same length, a Stephenson-II mechanism is obtained. In addition, if link B_0F (instead of link B_0B) is substituted by a parallel link of the same length, a Watt-I mechanism is obtained. For type A mechanisms, the size factor $\rho = 1$ and the link lengths are related by:

$$\overline{B_0F} = \overline{BG} = \overline{FE} = n\,\overline{B_0B} \quad \text{and} \quad \overline{FG} = \overline{B_0B} \qquad (4)$$

2.2.3 Construction of Type B Mechanisms.

For type B mechanisms as shown in Fig. 7, the embedded skew pantograph is B_0BFGEC. The construction of type B mechanisms is carried out through a procedure as follows:

1. Construct a four-bar linkage $A_0 - ABC - B_0$ such that $\overline{AB} = \overline{BC} = \overline{B_0B}$.
2. Reshape the binary link B_0B to a triangular plate B_0BF. (Similar to type A mechanisms, the choice of point F determines the amplification factor and the orientation of the output curve.)
3. Create a four-bar parallelogram $BCGF$ by adding two binary links CG and GF.
4. Reshape link FG to a triangular plate FGE such that ΔFGE is identical to ΔB_0BF.

Note that, type B mechanisms belong to Watt-I mechanisms and their link lengths are related by:

$$\overline{B_0F} = \overline{FE} = n\overline{B_0B}\ , \quad \overline{BF} = \overline{CG} = \overline{GE} = m\overline{B_0B}\ ,$$

$$\text{and} \quad \overline{FG} = \overline{B_0B} \tag{5}$$

3 MECHANISM CHARACTERISTICS

3.1 Six-Bar Linkages with an Embedded Regular Pantograph

Although type A and B mechanisms with an embedded regular pantograph are different in structure, the characteristics of their transmission angles and coupler curves are identical to each other.

3.1.1 Transmission Angle. Referring to the mechanisms shown in Fig. 3 or 4, the transmission angles of the four-bar linkage and the embedded regular pantograph are denoted as μ and ν, respectively. Although the singular condition [5] of such mechanisms can be avoided as long as μ and ν are kept between 0 and π, it is desirable to keep both of them as close to $\pi/2$ as possible. Thus, both transmission angles μ and ν should be constrained:

$$\epsilon < \mu < \pi - \epsilon \tag{6}$$

$$\epsilon < \nu < \pi - \epsilon \tag{7}$$

where ϵ is the minimum transmission angle for a mechanism to possess good force transmission characteristics. Usually, $\epsilon = 45°$ is assumed for both the four-bar linkage and the embedded regular pantograph.

According to Figs. 3 and 4, it is observed that the transmission angle ν of the embedded pantograph is determined by both the four-bar transmission angle μ and the coupler plate angle $\angle ABG$ (or ϕ). Since $0 < \mu < \pi$ and $0 < \phi < 2\pi$, we have $0 < \mu + \phi < 3\pi$. Referring to the mechanisms in Figs. 3(a), (b) or (c), the transmission angle ν can be expressed as

$$\nu = \begin{cases} \mu + \phi, & \text{for } 0 < \mu + \phi < \pi \\ 2\pi - (\mu + \phi), & \text{for } \pi < \mu + \phi < 2\pi \\ (\mu + \phi) - 2\pi, & \text{for } 2\pi < \mu + \phi < 3\pi \end{cases} \tag{8}$$

With the substitution of Eq. (8) into Eq. (7) and after simplification yields

$$\begin{aligned} &\text{(i)} \quad \epsilon - \phi < \mu < \pi - \epsilon - \phi, \\ &\qquad\qquad \text{for } 0 < \mu + \phi < \pi \\ &\text{(ii)} \quad \epsilon + (\pi - \phi) < \mu < \pi - \epsilon + (\pi - \phi), \\ &\qquad\qquad \text{for } \pi < \mu + \phi < 2\pi \\ &\text{(iii)} \ \epsilon + (2\pi - \phi) < \mu < \pi - \epsilon + (2\pi - \phi), \\ &\qquad\qquad \text{for } 2\pi < \mu + \phi < 3\pi \end{aligned} \tag{9}$$

[5] A singular condition refers to the condition when μ or ν is equal to 0 or π.

In order to satisfy both Eqs. (6) and (9), the transmission angle μ must fall in one of the following ranges:

$$\begin{aligned} &\text{(i)} \quad \epsilon < \mu < \pi - \epsilon - \phi, \\ &\qquad\qquad \text{for } 0 < \mu + \phi < \pi \\ &\text{(iia)} \ \epsilon + (\pi - \phi) < \mu < \pi - \epsilon, \\ &\qquad\qquad \text{for } \pi < \mu + \phi < 2\pi \text{ and } \pi - \phi \geq 0 \\ &\text{(iib)} \ \epsilon < \mu < \pi - \epsilon + (\pi - \phi), \\ &\qquad\qquad \text{for } \pi < \mu + \phi < 2\pi \text{ and } \pi - \phi < 0 \\ &\text{(iii)} \ \epsilon + (2\pi - \phi) < \mu < \pi - \epsilon, \\ &\qquad\qquad \text{for } 2\pi < \mu + \phi < 3\pi \end{aligned} \tag{10}$$

Comparing the admissible range of μ in Eq. (10) for a six-bar mechanism with an embedded regular pantograph with that in Eq. (6) for a four-bar mechanism, we observe that the admissible ranges of μ for the four-bar linkages have been reduced by an amount of ϕ, $|(\pi - \phi)|$, and $(2\pi - \phi)$ for cases (i) through (iii), respectively. Such a reduction in the range of μ may be considered as a significant design limitation.

3.1.2 Coupler-Point Curve. The coupler curve of a six-bar mechanism with an embedded regular pantograph satisfies the following theorem.

Theorem 1. *Referring to the six-bar mechanisms in Fig. 3 or 4, the amplified coupler curve generated by point E is bounded between two concentric circles centered at B_0 and with radii of $(\overline{B_0E})_{\alpha=0}$ and $(\overline{B_0E})_{\alpha=\pi}$, where*
(i) $(\overline{B_0E})_{\alpha=\pi} > (\overline{B_0E})_{\alpha=0}$, if $0 < \mu + \phi < \pi$ or $2\pi < \mu + \phi < 3\pi$, or
(ii) $(\overline{B_0E})_{\alpha=0} > (\overline{B_0E})_{\alpha=\pi}$, if $\pi < \mu + \phi < 2\pi$.

Proof. Referring to Fig. 3(b), $\overline{B_0E}$ can be obtained by applying the cosine law to ΔB_0EF,

$$\overline{B_0E} = \sqrt{2}\ \overline{B_0F}\,(1 - \cos\nu)^{1/2} \tag{11}$$

Since $\cos\nu$ is a monotonically decreasing function within the range of $0 < \nu < \pi$, the maximum and minimum of $\overline{B_0E}$ occur at $\nu = \nu_{\max}$ and $\nu = \nu_{\min}$, respectively.

(i) For $0 < \mu + \phi < \pi$ or $2\pi < \mu + \phi < 3\pi$, we observe from Eq. (8) that the maximum and minimum values of ν follow that of μ. Hence, $\nu_{\max}$ and $\mu_{\max}$ occur at $\alpha = \pi$; $\nu_{\min}$ and $\mu_{\min}$ occur at $\alpha = 0$. This, in turn, indicates that $(\overline{B_0E})_{\alpha=\pi}$ and $(\overline{B_0E})_{\alpha=0}$ are the longest and the shortest distances between points E and B_0 for $\alpha \in [0, 2\pi]$.

(ii) Similarly, for $\pi < \mu + \phi < 2\pi$ we observe from Eq. (8) that the maximum value of ν follows the minimum value of μ and vice versa. Hence, $\nu_{\max}$ and $\mu_{\min}$ occur at

$\alpha = 0$; $\nu_{\min}$ and $\mu_{\max}$ occur at $\alpha = \pi$. This indicates that $(\overline{B_0E})_{\alpha=0}$ and $(\overline{B_0E})_{\alpha=\pi}$ are the longest and the shortest distances between points E and B_0 for $\alpha \in [0, 2\pi]$.

From (i) and (ii), we conclude that the entire coupler curve is bounded between two concentric circles centered at B_0 and with radii of $(\overline{B_0E})_{\alpha=\pi}$ and $(\overline{B_0E})_{\alpha=0}$, respectively. □

3.2 Six-Bar Linkages with an Embedded Skew Pantograph

For this class of six-bar mechanisms, the transmission angle characteristics between type A and type B mechanisms are different, while the characteristics of their coupler curves remain identical to each other.

3.2.1 Transmission Angle of Type A Mechanism.

Referring to the type A mechanisms shown in Fig. 6, the transmission angles of the four-bar linkage and the embedded skew pantograph are denoted as μ and ν', respectively. Similar to the six-bar mechanisms with an embedded regular pantograph, these transmission angles should be constrained:

$$\epsilon < \mu < \pi - \epsilon \tag{12}$$

$$\epsilon < \nu' < \pi - \epsilon \tag{13}$$

Referring to Fig. 8, the value of transmission angle ν' of the embedded skew pantograph is determined by both μ and the coupler plate angle $\angle ABG$. The value of $\angle ABG$ depends on the angle $\angle ABC$ and the relative orientation angle between $\overrightarrow{B_0F}$ and $\overrightarrow{B_0H}$ (or $\overrightarrow{B_0C}$). For instance, if the orientation of $\overrightarrow{B_0F}$ is achieved by rotating the vector $\overrightarrow{B_0H}$ clockwise about B_0 through an angle ψ_2 as shown in Fig. 8(a), then $\angle ABG = \angle ABC + \angle CBG = \phi + \psi_2$. Otherwise, if the orientation of $\overrightarrow{B_0F}$ is achieved by rotating the vector $\overrightarrow{B_0H}$ counter-clockwise about B_0 through an angle ψ_2 as shown in Fig. 8(b), then $\angle ABG = \angle ABC - \angle GBC = \phi - \psi_2$. Hence, denoting $\angle ABG$ as ϕ' yields

$$\phi' = \phi + a\psi_2 \tag{14}$$

where $a = \pm 1$. Note that, the coupler curve at E is obtained by rotating the curve at C clockwise or counter-clockwise about point B_0 through an angle ψ_2 according to $a = 1$ or $a = -1$. (see Figs. 8(a) and (b))

Since $0 < \mu < \pi$ and $0 < \phi < 2\pi$, we have $0 < \mu + \phi + a\psi_2 < 3\pi + a\psi_2$ or $0 < \mu + \phi' < 3\pi + a\psi_2$. Referring to the mechanisms in Figs. 6(a), (b) or (c), the transmission

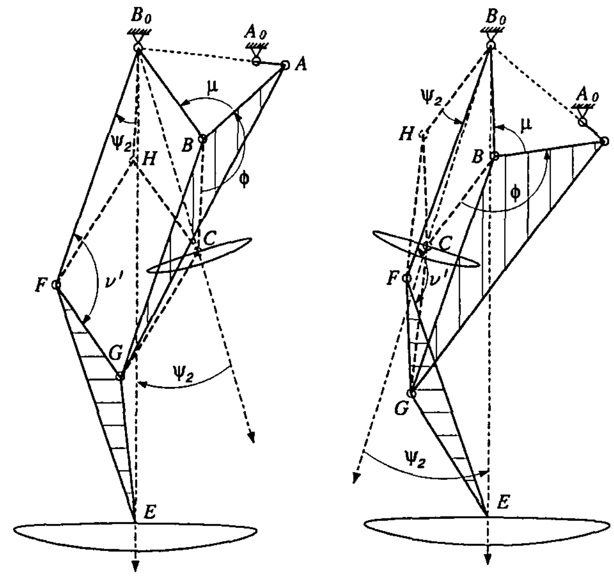

(a) (b)

Figure 8. Coupler curve at C is rotated about point B_0 through an angle ψ_2 at point E: (a) clockwise rotation ($a = +1$) and (b) counter-clockwise rotation ($a = -1$)

angle ν' of the embedded pantograph can be expressed as

$$\nu' = \begin{cases} \mu + \phi', & \text{for } 0 < \mu + \phi' < \pi \\ 2\pi - (\mu + \phi'), & \text{for } \pi < \mu + \phi' < 2\pi \\ (\mu + \phi') - 2\pi, & \text{for } 2\pi < \mu + \phi' < 3\pi \end{cases} \tag{15}$$

Note that, since the condition $\mu + \phi' > 3\pi$ is not desirable, such a condition is not considered. Substituting Eq. (15) into (13) and satisfying Eq. (12), the transmission angle μ of type A mechanisms must fall in either of the following ranges:

$$\begin{array}{ll} \text{(i)} & \epsilon < \mu < \pi - \epsilon - \phi', \\ & \quad \text{for } 0 < \mu + \phi' < \pi \\ \text{(iia)} & \epsilon + (\pi - \phi') < \mu < \pi - \epsilon, \\ & \quad \text{for } \pi < \mu + \phi' < 2\pi \text{ and } \pi - \phi' \geq 0 \\ \text{(iib)} & \epsilon < \mu < \pi - \epsilon + (\pi - \phi'), \\ & \quad \text{for } \pi < \mu + \phi' < 2\pi \text{ and } \pi - \phi' < 0 \\ \text{(iii)} & \epsilon + (2\pi - \phi') < \mu < \pi - \epsilon, \\ & \quad \text{for } 2\pi < \mu + \phi' < 3\pi \end{array} \tag{16}$$

Eq. (16) shows that, when compared with a four-bar linkage, the admissible range of μ for type A mechanism is reduced by an amount of ϕ', $|(\pi - \phi')|$, and $(2\pi - \phi')$ for ranges (i) through (iii), respectively. Since $\phi' = \phi + a\psi_2$

and $a = \pm 1$, the admissible range of μ for a mechanism with an embedded skew pantograph is larger than that with an embedded regular pantograph, if the value of a is selected as -1, $+1$, -1, and $+1$ for cases (i), (iia), (iib), and (iii), respectively.

3.2.2 Transmission Angle of Type B Mechanism.

Referring to type B mechanisms shown in Fig. 7, the transmission angle ν'' of the embedded skew pantograph can be expressed as

$$\nu'' = \begin{cases} \mu + \phi'', & \text{for } 0 < \mu + \phi'' < \pi \\ 2\pi - (\mu + \phi''), & \text{for } \pi < \mu + \phi'' < 2\pi \\ (\mu + \phi'') - 2\pi, & \text{for } 2\pi < \mu + \phi'' < 3\pi \end{cases} \tag{17}$$

where

$$\phi'' = \phi - a\psi_1 - a\psi_2 \tag{18}$$

and $a = \pm 1$. Note that, for the mechanisms in Fig. 7, we have $a = +1$.

For this type of mechanisms, since $\phi'' = \phi - a\psi_1 - a\psi_2$ and $a = \pm 1$, the admissible range of μ for a mechanism with an embedded skew pantograph will be larger than that with an embedded regular pantograph, if the value of a is properly selected.

3.2.3 Coupler-Point Curve.

Referring to type A mechanism as shown in Fig. 6, the distance between the fixed point B_0 and the output point E can be written as

$$\overline{B_0E} = \sqrt{2}\ \overline{B_0F}\,[1 - \cos(\angle B_0FE)]^{1/2} \tag{19}$$

where $0 < \angle B_0FE < \pi$. Since $\angle B_0FE$ can be written as

$$\angle B_0FE = \nu' + \begin{cases} -a\psi_2, & \text{for } 0 < \mu + \phi' < \pi \\ +a\psi_2, & \text{for } \pi < \mu + \phi' < 2\pi \\ -a\psi_2, & \text{for } 2\pi < \mu + \phi' < 3\pi \end{cases} \tag{20}$$

Substituting Eq. (15) into (20) yields

$$\angle B_0FE = \begin{cases} \mu + \phi, & \text{for } 0 < \mu + \phi' < \pi \\ 2\pi - (\mu + \phi), & \text{for } \pi < \mu + \phi' < 2\pi \\ (\mu + \phi) - 2\pi, & \text{for } 2\pi < \mu + \phi' < 3\pi \end{cases} \tag{21}$$

In Eq. (21), it is possible that the maximum value of $\angle B_0FE$ is greater than π and the minimum value of $\angle B_0FE$

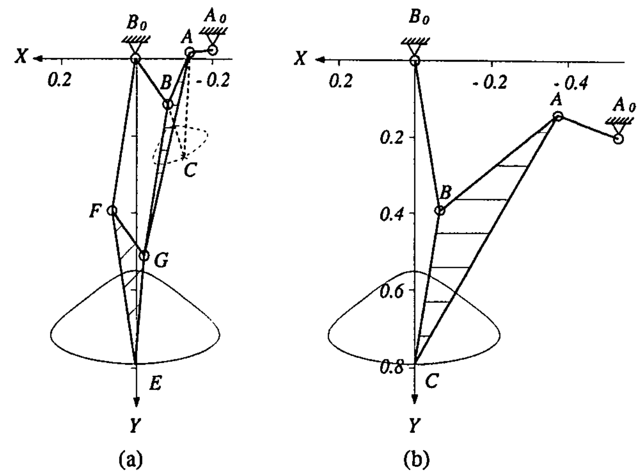

Figure 9. An identical coupler curve generated by (a) a six-bar mechanism with an embedded skew pantograph (b) a four-bar linkage

is less than 0. Hence, the maximum and minimum values of $\overline{B_0E}$ may not occur at the crank angle $\alpha = 0$ or $\alpha = \pi$. Therefore, Theorem 1 no longer holds for type A six-bar mechanisms with an embedded skew pantograph. Similarly, it can be shown that Theorem 1 does not hold for type B mechanisms.

4 EXAMPLE MECHANISM

Fig. 9(a) shows a six-bar mechanism with an embedded skew pantograph. Since this mechanism is designed with $\overline{AB} = \overline{B_0B} = \overline{BC}$, point C traces a symmetrical coupler-point curve while crank A_0A rotates about the fixed pivot A_0. By using the additional dyad B_0FGE to form an embedded skew pantograph, the coupler curve at point C is amplified by a factor of $n = \overline{B_0F}/\overline{B_0B}$ and is rotated clockwise about point B_0 through an angle of $\angle GFE$. Fig. 9(b) shows a four-bar linkage which generates a coupler curve identical to that of the six-bar mechanism. For the purpose of comparison, two X-Y reference coordinate systems with their Y-axes pointing downward along the line of symmetry and with their origins located at joint B_0 are defined in Figs. 9(a) and (b). It is clear that, when an identical curve is traced, the six-bar linkage shown in Fig. 9(a) is more compact than the four-bar mechanism shown in Fig. 9(b). Such a compactness is important in many applications, especially for a multi-legged walking machine where the interference between adjacent legs is crucial.

5 CONCLUDING REMARKS

We have presented a new class of six-bar mechanisms which are capable of generating relatively large symmetrical coupler curves at their output points. The basic idea behind the development of these mechanisms is to combine the functions of a four-bar linkage and a pantograph into one. For such mechanisms, the four-bar linkage generates a symmetrical coupler curve which is then amplified via an embedded regular or skew pantograph to a desired size. As such, the analysis or synthesis of these mechanisms can be easily performed beginning with the four-bar linkage and followed by the pantograph.

It is shown that the six-bar mechanisms in this class can be constructed in two different types (or structures). For those mechanisms with an embedded regular pantograph, both types of mechanisms are subject to the same transmission angle constraints. However, for those mechanisms with an embedded skew pantograph, the two types of mechanisms yield different transmission characteristics. The characteristics of the six-bar coupler curves are also investigated. Because of the different characteristics, six-bar mechanisms with an embedded skew pantograph are shown to exhibit better design flexibility. Finally, an example of a six-bar mechanism from this class is shown to be more compact than a four-bar, when an identical coupler curve is traced.

ACKNOWLEDGMENT

The work was supported in part by the National Science Foundation, Grant No. EID-9212126. Such a support does not constitute an endorsement of the opinions expressed in the paper by the funding agency.

REFERENCES

Antuma, H. J., 1978, "Triangular Nomograms for Symmetrical Coupler Curves," Mechanism and Machine Theory, Vol. 13, No. 3, pp. 251–267.

Dijksman, E., 1976, *Motion Geometry of Mechanisms*, Cambridge University Press, 4th Eds., London, UK.

Dijksman, E. A., 1979, "Symmetrical Coupler Curves, Produced by a 6-Bar Linkage of Type Stephenson-I," *Proceedings of Fifth World Congress on Theory of Machine and Mechanism*, pp. 537–540.

Dijksman, E. A., 1980a, "Half-Symmetrical 6-Bar Curves Produced by Focal Linkages or Their Derivatives," Mechanism and Machine Theory, Vol. 15, No. 3, pp. 221–228.

Dijksman, E. A., 1980b, "Highest-Order Coupler Points of Watt-I Linkages, Tracing Symmetrical 6-Bar Curves," Mechanism and Machine Theory, Vol. 15, No. 6, pp. 421–434.

Dijksman, E. A., 1981, "Watt-I Linkages with Shunted Chebyshev-Dyads, Producing Symmetrical 6-Bar Curves," Mechanism and Machine Theory, Vol. 16, No. 2, pp. 153–165.

Dijksman, E. A., 1984, "An Unsymmetrical Watt-I Linkage Generating A Family of Symmetrical Curves," Mechanism and Machine Theory, Vol. 19, No. 3, pp. 297–306.

Funabashi, H., Ogawa, K., Gotoh, Y., and Kojima, K., 1985, "Synthesis of Leg-Mechanisms of Biped Walking Machines (Part I, Synthesis of Ankle-Path-Generator)," Bulletin of JSME, Vol. 28, No. 237, pp. 537–543.

Hartenberg, R., and Denavit, J., 1964, *Kinematics Synthesis of Linkages*, McGraw-Hill Inc., New York, New York.

Shieh, W. B., Tsai, L. W., Azarm, S., and Tits, A. L., 1995, "Multiobjective Optimization of a Leg Mechanism with Various Spring Configurations for Force Reduction,". Advances in Design Automation, DE-Vol. No. 82, ASME Pub., pp. 811-818 (also, accepted in the Trans. ASME, Journal of Mechanical Design).

Song, S. M., Lee, J. K., and Waldron, K. J., 1987, "Motion Study of Two- and Three-Dimensional Pantograph Mechanisms," Mechanism and Machine Theory, Vol. 22, No. 4, pp. 321–331.